Application of Traditional and Novel Cloud Property Retrieval Techniques on Landsat TM Data over SGP

L. Oreopoulos, R. F. Cahalan, A. Marshak, and G. Wen
Climate and Radiation Branch, NASA-Goddard Space Flight Center
Greenbelt, Maryland
Joint Center for Earth Systems Technology, University of Maryland, Baltimore County
Baltimore, Maryland

Introduction

With the recognition in recent years of the influence of three-dimensional (3-D) radiative transfer on cloud optical property retrievals, interest in the measurements of the Thematic Mapper (TM) radiometer aboard the Landsat satellite has been renewed. This instrument provides a unique high-resolution data set where the effects of 3-D cloud structure are expected to be prominent. The purpose of this paper is to examine the real world application of the Nonlocal Independent Pixel Approximation (NIPA) of Marshak et al. (1998), and to suggest a new Independent Pixel Approximation (IPA) using normalized reflectivity differences. Our satellite data set consists of a full Landsat scene over the Atmospheric Radiation Measurement (ARM) Program's Southern Great Plains (SGP) site.

Satellite Data Set

The satellite image used in this paper is from the TM instrument aboard Landsat-5, and covers an area of ~196 km^2 x 185 km^2 at a resolution of 28.5 m around the ARM SGP site. The time of the satellite overpass was 16:25 Greenwich Mean Time (GMT) on September 24, 1996. The solar zenith angle (SZA) at that time was ~45° and the azimuth angle (AZA) was 138°. We use various TM bands to establish thresholds for distinguishing between clear and cloudy pixels, and look-up tables of band 4 (B4-0.83 μm) and band 7 (B7-2.2 μm) to retrieve cloud optical depth (τ), effective radius (re), and liquid water path (LWP). The retrieval procedure is described elsewhere (Oreopoulos et al. 1999).

IPA, NDNR, and NIPA Retrievals

As discussed in Stephens (1988), Marshak et al. (1998), Davis et al. (1997), and others, net horizontal transfer of photons between pixels tends to smooth fields of reflected solar radiation and results in the underestimation of retrieved optical depth variability. The spatial scale at which this takes place depends on the SZA and the wavelength of the incident radiation. When SZA exceeds ~35° to 40°, roughening starts taking place (Zuidema and Evans 1998; Várnai 1999), which is more prominent at absorbing wavelengths and can be seen in intermediate scales (~1 km to 2 km) of Landsat power spectra. Roughening results in overestimates of retrieved optical depth variability (Várnai 1999). Thus, the optimal reconstruction of IPA nadir reflectivity fields to be inverted could potentially involve a) roughening at small scales, b) smoothing at intermediate scales, and c) accounting for wavelength

(absorption) dependencies. A possible approach for b) is retrievals using normalized differences of nadir reflectivity (NDNR), as discussed below. For a) the inverse NIPA of Marshak et al. (1998) is appropriate. The theoretical and empirical background to tackle c) is still under development. In the following, we will concentrate on a) and b).

NDNR

Marshak et al. (1999) have argued that shadowing and side illumination at low sun angles affect nadir transmissivities as observed from the ground under broken cloud conditions. They claim that these 3-D effects are similar for conservative and moderately absorbing wavelengths, and absent to a large degree in a normalized difference transmissivity ratio, which can then be used to retrieve optical depths. Here, we similarly use the NDNR of a conservative and an absorptive wavelength as a tool for potential removal of intermediate scale roughening. Initially, the performance of NDNR will be demonstrated using nadir reflectivities at SZA = 60° from 3-D Monte Carlo (MC) simulations on a one-dimensional (1-D) optical depth field generated with the bounded cascade cloud model of Cahalan et al. (1994). More information on the optical depth field is given in the caption of Figure 1. Note that the NDNR retrievals tend to smooth the optical depth field in a manner similar to that of the IPA retrievals at high SZAs (Marshak et al. 1998; Figure 1b), but gives better statistics than the IPA, which retrieves a very rough apparent optical depth field. Although these results do not include atmospheric effects or reflective ground surfaces, an extended NDNR = (R4-R7)/(R4+R7) constructed from the Landsat look-up tables (which include atmosphere and surface effects) can also be inverted because NDNR remains a monotonic function of visible optical depth (not shown).

Figure 2a shows that the retrievals from the (NDNR, B7) pair give an optical depth histogram that is very similar to that of the (B4, B7) pair. While this is expected for effective radius retrievals (Figure 2b), it is somewhat surprising for the optical depth retrievals. However, further analysis reveals that despite the similarity of the histograms, pixel-level optical property depth differences are non-trivial: Figure 3 shows root mean square (rms) differences for 25 subscenes (of size 1024 x 1024 pixels) into which the original scene was divided. For some subscenes, rms differences exceed 3 for optical depth, while effective radius rms are small (as expected) with the exception of the first few subscenes where broken clouds are numerous. The overall rms for the entire scene is 2.30 for optical depth and 1.39 μm for effective radius. In the following, we will show that NDNR can be combined with NIPA in a new retrieval algorithm. This is strictly justifiable only when NDNR-retrieved fields are smoother than their IPA counterparts. The subscene results do not consistently support this (NDNR-retrieved standard deviations occasionally exceed IPA-retrieved not shown), nor does the overall histogram of Figure 2a. This inconsistency may be due to imprecise modeling of surface and atmospheric effects.

Figure 4 compares the IPA and NDNR retrievals for the topmost 2000 scanlines of the scene (which contain the Cloud and Radiation Testbed [CART] facility) with the Microwave Radiometer (MWR) values of LWP. In this comparison, we have discarded values <20 gm^{-2} for both satellite retrievals and surface measurements, and renormalized the histograms with respect to the remaining values. The rationale is that there is a residual error of the multiple linear regression used to convert MWR brightness temperatures to LWP and this sets a threshold (~20 gm^{-2}) for unambiguous cloud detection.

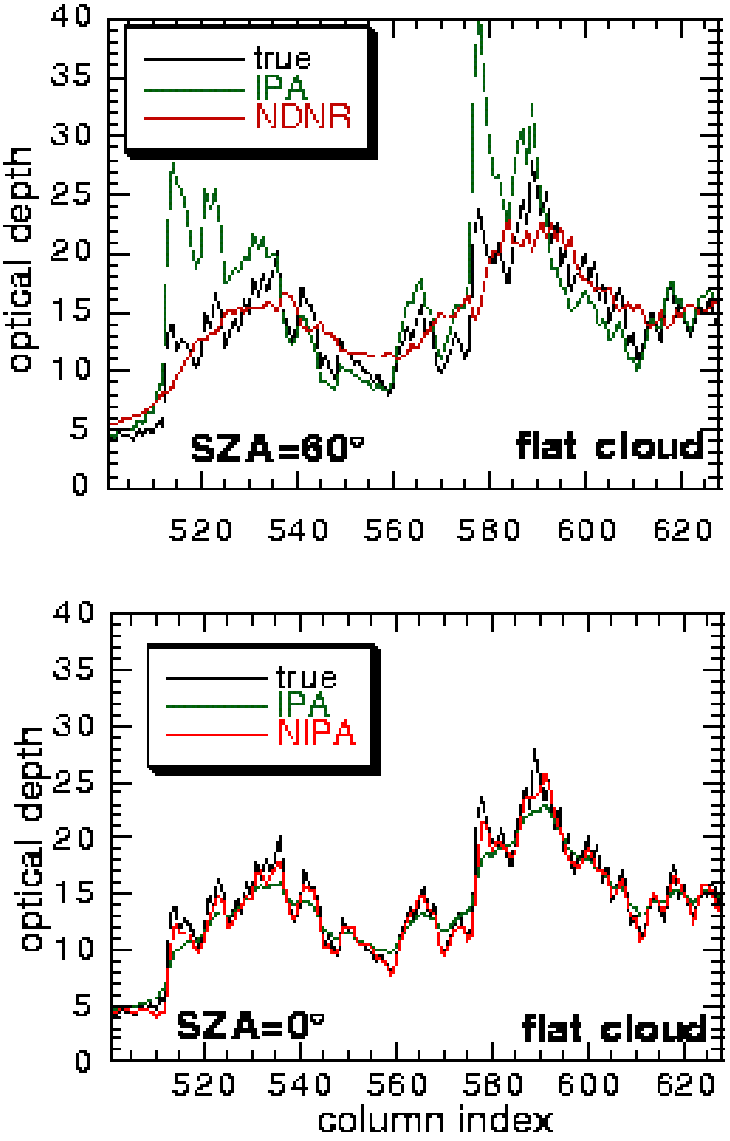

Figure 1. Comparison of IPA and NDNR/NIPA - retrieved cloud optical depth using MC nadir reflectivities ($\omega 0$ = 0.98 for the absorbing band in NDNR) with the true optical depth. The figure shows a 128-column segment from a 1024-column optical depth field generated with the bounded cascade model (Cahalan et al. 1994). Cascade parameters are p = 0.3, H = 0.33, column width is 25 m. The sun is shining from left when SZA = 60°. The cloud is flat with thickness 0.3 km, surface is black, and there are no atmospheric effects. A Henyey-Greenstein phase function with g = 0.85 was used in a 2 x 108 photon simulation. The NIPA parameters were η = 0.09, α = 1.0, γ = 0.002.

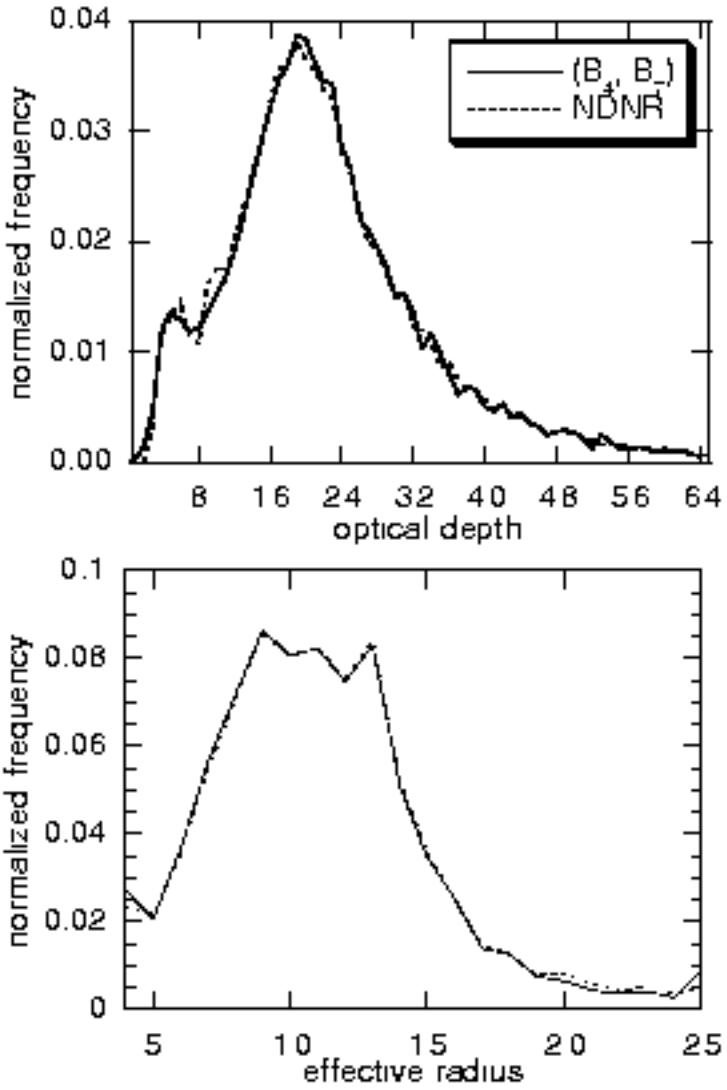

Figure 2. Comparison of the (B4, B7) optical depth and effective radius (μm) histograms with the corresponding (NDNR, B7) histograms.

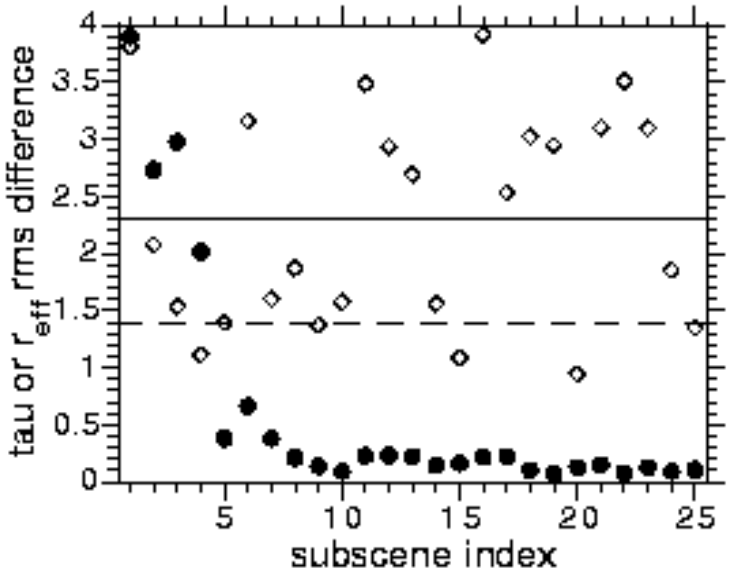

Figure 3. Root mean square differences between optical depths (diamonds) and effective radii (circles) retrieved from (B4, B7) and (NDNR, B7) for 1024x1024 subscenes into which the original scene was divided. The overall rms difference for the entire scene is shown by the solid line for optical depth (2.29) and the dashed line for effective radius (1.39 μm).

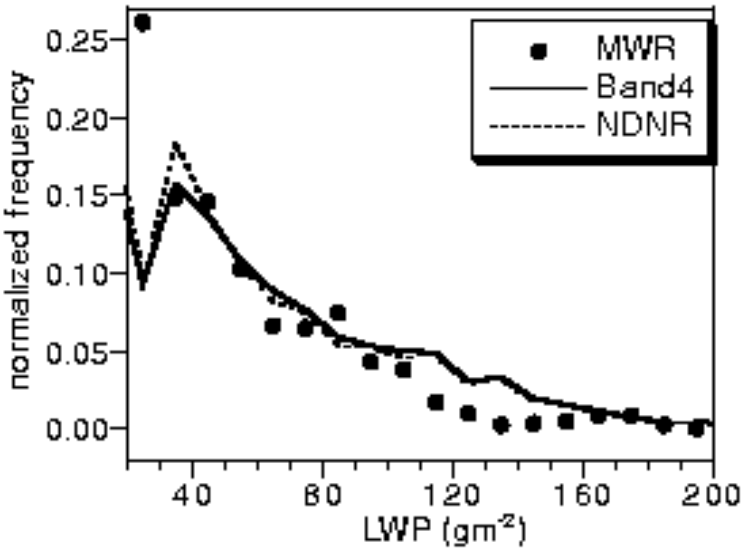

Figure 4. LWP histogram comparison between MWR-derived values around the time of satellite overpass, and Landsat-derived values for the topmost 2000 scanlines from (NDNR, B7) and (B4, B7) retrievals.

NIPA

Figure 1b shows application of NIPA on the cascade cloud (as in Marshak et al. 1998). We also have applied inverse NIPA on the observed B4 and B7 radiances of several 256 x 256 overcast segments of our Landsat scene, and proceeded to optical depth and effective radius retrievals as before. Figure 5 compares the (B4, B7) optical depth field retrieved from IPA and NDNR with several incarnations of NIPA for one of these subscenes. These incarnations result from different values of the parameters α, η of the NIPA kernel (a gamma distribution approximating the distribution of distances photons travel from their entry point; see Marshak et al. 1998) involved in the transformation. γ is a parameter of the regularization function introduced because of the "ill-posed" nature of the inverse problem (Marshak et al. 1998). The NIPA transformation does indeed lead to more variable optical depth fields, but there is a sensitivity to the choice of the regularization parameter γ (a fact stressed by Marshak et al. 1998). If γ is changed to a tenth of its Figure 5 value NIPA will give smoother instead of rougher fields. For parameter values $\eta = 0.025$, $\alpha = 0.5$, the standard deviation $\sigma\tau$ of the optical depth field is 7.36 compared to 6.87 for IPA. $\sigma\tau$ increases to 8.18 for $\eta = 0.035$, $\alpha = 0.5$ and is 8.04 for $\eta = 0.025$, $\alpha = 1.0$. From the above, it is obvious that increasing either η or α results in rougher reflectivity and optical depth fields. Note that none of the above transformations affects significantly the mean value of optical depth (~24).

NDNR-NIPA

Since there is evidence from simulations that NDNR retrievals behave similarly to IPA retrievals for high sun (Figure 1), it would seem appropriate to apply inverse NIPA to compensate for smoothing. The NDNR-IPA optical depth field is compared with a realization of the corresponding NDNR-NIPA field in Figure 5. The effect of NIPA is similar on NDNR retrievals as on the standard (B4, B7) retrievals: $\sigma\tau$ increases from 7.28 for IPA-NDNR to 8.31 for NIPA-NDNR. The most interesting point is that there is a greater amount of roughening induced by identical NIPA parameters when applied on NDNR compared to B4 (not shown). We plan to conduct more MC simulations to investigate whether there is a clear winner between the two NIPA transformations.

Conclusions

We have introduced NDNR = (R4-R7)/(R4+R7) as a new quantity to be used for IPA-type optical depth retrievals. We showed using MC simulations that NDNR retrievals at oblique sun illuminations perform better than IPA retrievals, eliminating extrema in optical depth and giving better statistics. We suggested that NDNR retrievals at low sun are similar in character to standard IPA retrievals at high sun. When NDNR was applied to Landsat data we found that they do not affect significantly overall statistics and histograms of optical properties, but introduce important differences at the pixel level (especially for optical depth). NIPA was applied for the first time on satellite observations (in this case overcast 256 x 256 pixel subregions of the Landsat scene), and the dependence of the degree of roughening on the parameters of the NIPA kernel was demonstrated. It was also shown that retrievals using a combination of NIPA and NDNR are feasible.

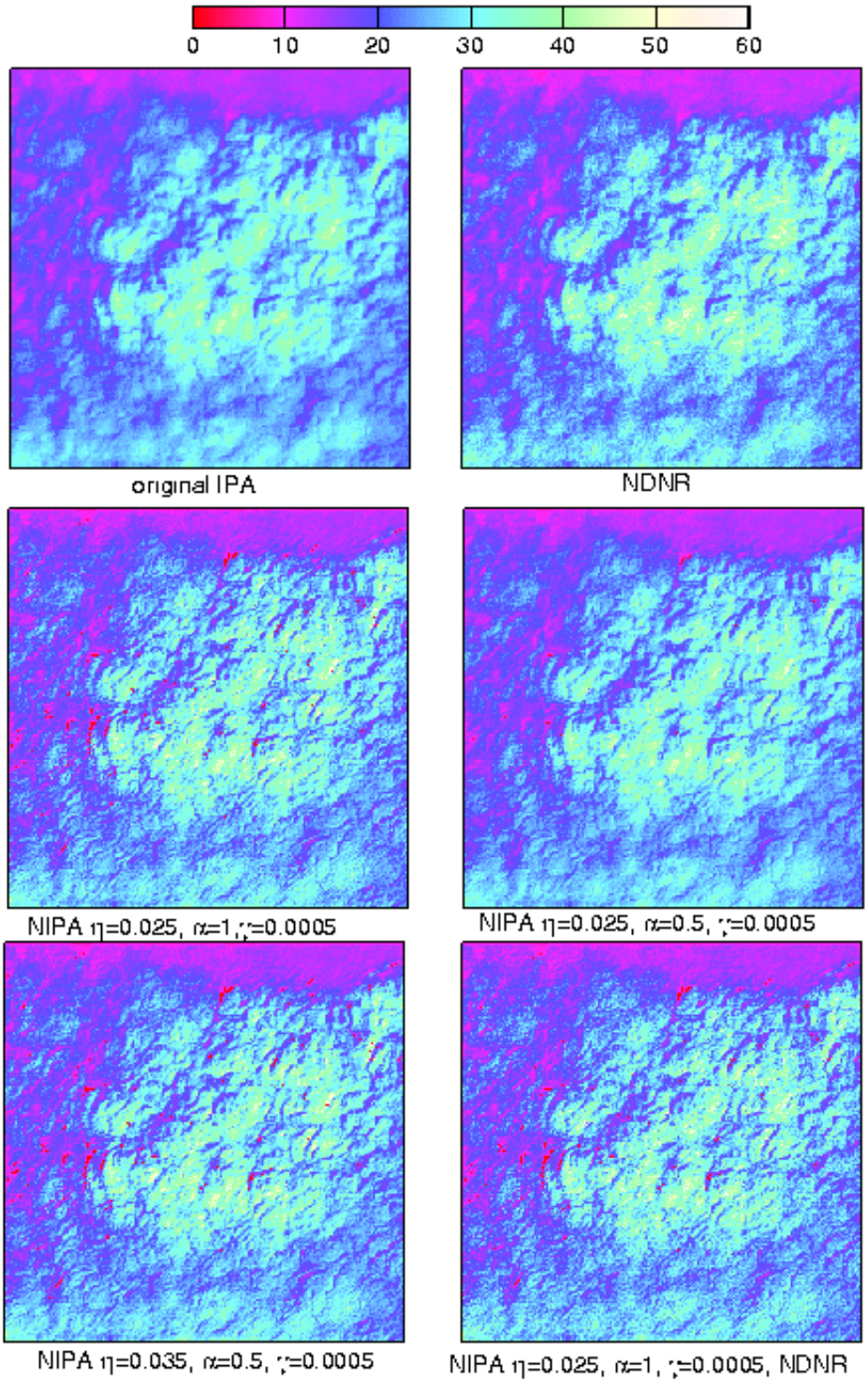

Figure 5. Retrieved optical depths (using B4) for IPA, NDNR, various NIPA, and a NDNR-NIPA case for an overcast 256 x 256 region of the Landsat scene.

Clearly, NIPA, NDNR, and a potential hybrid scheme are concepts still in their prepubescent stages. The dependencies of the NIPA parameters and the procedure for tracking down their optimal values is still under development. The suitability of NIPA-type extensions for partially cloudy fields and NDNR difficulties for optically thin clouds have yet to be closely examined. We are currently performing extensive MC simulations to address these issues.

References

Cahalan, R. F., W. Ridgway, W. J. Wiscombe, T. L. Bell, and J. B. Snider, 1994: The albedo of fractal stratocumulus clouds. *J. Atmos. Sci.*, **51**, 2434-2455.

Davis, A., A. Marshak, R. F. Cahalan, and W. J. Wiscombe, 1997: The Landsat scale break in stratocumulus as a three-dimensional radiative transfer effect: Implications for cloud remote sensing. *J. Atmos. Sci.*, **54,** 241-260.

Marshak, A., A. Davis, R. F. Cahalan, and W. J. Wiscombe, 1998: Nonlocal independent pixel approximation: Direct and inverse problems. *IEEE Trans. Geosc. Rem. Sens.*, **36**, 192-205.

Marshak, A., Y. Knyazikhin, A. Davis, W. J. Wiscombe, and J. Barnard, 1999: Clouds - vegetation interaction; the use of two-channels narrow field of view (NFOV) radiometer for the independent estimate of cloud optical thickness. This proceedings.

Oreopoulos, L., R. F. Cahalan, A. Marshak, and G. Wen, 1999: Application of traditional and novel cloud optical property techniques on Landsat and ARM data, and Monte Carlo simulations. *J. Appl. Meteor.* Submitted.

Stephens, G. L., 1988: Radiative transfer through arbitrary shaped optical media, Part 1 A general method of solution. *J. Atmos. Sci.*, **45**, 1818-1836.

Várnai, T., 1999: Influence of three-dimensional radiative effects on the spatial distribution of shortwave cloud reflection. *J. Atmos. Sci.* In press.

Zuidema, P., and K. F. Evans, 1998: On the validity of the independent pixel approximation for boundary layer clouds observed during ASTEX. *J. Geophys. Res.*, **103**, 6059-6074.